Published in final edited form as:
*Remote Sens Environ*. 2012 October ; 125: 147–156. doi:10.1016/j.rse.2012.07.018.

# Satellite Microwave Remote Sensing for Environmental Modeling of Mosquito Population Dynamics

**Ting-Wu Chuang**[1,*], **Geoffrey M. Henebry**[1], **John S. Kimball**[2], **Denise L. VanRoekel-Patton**[3], **Michael B. Hildreth**[4,5], and **Michael C. Wimberly**[1]

[1]Geographic Information Science Center of Excellence, South Dakota State University, Brookings, SD 57007, United States

[2]Flathead Lake Biological Station, Division of Biological Sciences, The University of Montana, Polson, MT 59860, United States

[3]City of Sioux Falls Health Department, Sioux Falls, SD 57104, United States

[4]Department of Biology and Microbiology, South Dakota State University, Brookings, SD 57007, United States

[5]Department of Veterinary & Biomedical Science, South Dakota State University, Brookings, SD 57007, United States

## Abstract

Environmental variability has important influences on mosquito life cycles and understanding the spatial and temporal patterns of mosquito populations is critical for mosquito control and vector-borne disease prevention. Meteorological data used for model-based predictions of mosquito abundance and life cycle dynamics are typically acquired from ground-based weather stations; however, data availability and completeness are often limited by sparse networks and resource availability. In contrast, environmental measurements from satellite remote sensing are more spatially continuous and can be retrieved automatically. This study compared environmental measurements from the NASA Advanced Microwave Scanning Radiometer on EOS (AMSR-E) and *in situ* weather station data to examine their ability to predict the abundance of two important mosquito species (*Aedes vexans* and *Culex tarsalis*) in Sioux Falls, South Dakota, USA from 2005 to 2010. The AMSR-E land parameters included daily surface water inundation fraction, surface air temperature, soil moisture, and microwave vegetation opacity. The AMSR-E derived models had better fits and higher forecasting accuracy than models based on weather station data despite the relatively coarse (25-km) spatial resolution of the satellite data. In the AMSR-E models, air temperature and surface water fraction were the best predictors of *Aedes vexans*, whereas air temperature and vegetation opacity were the best predictors of *Cx. tarsalis* abundance. The models were used to extrapolate spatial, seasonal, and interannual patterns of climatic suitability for mosquitoes across eastern South Dakota. Our findings demonstrate that environmental metrics derived from satellite passive microwave radiometry are suitable for predicting mosquito population dynamics and can potentially improve the effectiveness of mosquito-borne disease early warning systems.



[*]Corresponding Author Address correspondence to Ting-Wu Chuang, Geographic Information Science Center of Excellence, South Dakota State University, 1021 Medary Ave., Wecota Hall, Brookings, SD 57007, United States Phone: +1-605-688-5856 Fax: +1-605-688-5227 Ting-Wu.Chuang@sdstate.edu.

**Keywords**

AMSR-E; Weather Station; West Nile Virus; Mosquito; Public Health

## 1. Introduction

Vector-borne disease is responsible for more morbidity and mortality in humans than any other type of infectious disease, and the mosquito is one of the most important vectors (Gubler, 1998). More than 300 million cases of malaria and 50–100 million cases of dengue are reported worldwide every year, highlighting the enormous global public health impact of mosquito-borne diseases (WHO, 2009a, 2009b). West Nile virus (WNV) has become the most significant mosquito-borne disease in North America after its entry into the continent in 1999 and currently has the broadest global geographic distribution of any contemporary vector-borne disease (Hofmeister, 2011). Mosquito-borne diseases are sensitive to various environmental factors that influence pathogen, vector, and host ecology. Remotely-sensed environmental monitoring data, primarily in the visible and infrared spectra, have been widely applied to map and forecast vector-borne diseases at spatial scales ranging from landscapes to the entire globe (Adimi et al., 2010; Hay & Lennon, 1999; Machault et al., 2010). In contrast, other types of earth observation data, such as passive microwave radiometry, have been greatly underutilized in public health applications despite microwave sensitivity to surface moisture, temperature and vegetation characteristics that may provide effective surrogates for environmental controls influencing mosquito habitat and life cycle dynamics. Therefore, the main goal of our study was to assess the potential for modeling mosquito population dynamics using environmental variables derived from satellite passive microwave radiometry.

Mosquito-borne disease transmission is closely linked with mosquito behavior and population dynamics (Bolling et al., 2009; Ebel et al., 2005). In particular, temperature and humidity influence the larval developmental rate, the length of the gonotrophic cycle, mosquito survival, and the extrinsic incubation period (EIP); and sufficient rainfall is necessary to create and maintain larval habitats (Becker et al., 2003). Meteorological data from weather stations is frequently used to investigate mosquito abundances and disease risk (Chuang et al., 2011; Kristan et al., 2008; Trawinski & Mackay, 2008). These data provide direct measurements of near-surface ambient temperature, precipitation, relative humidity, wind speed, and atmospheric pressure. However, the distribution of weather stations is not homogeneous and can be very sparse in rural areas and in most developing countries. Data collection and equipment maintenance is labor intensive and costly resulting in incomplete data records, particularly in the developing world.

Satellite remote sensing techniques provide an alternative source of environmental data that are being increasingly applied to assess the risk of vector-borne diseases and vector population dynamics (Beck et al., 2000; Kalluri et al., 2007). In contrast to weather stations, remote sensing data provide spatially continuous and automated global measurements of a diverse range of environmental information. For example, the normalized difference vegetation index (NDVI) in combination with land surface temperature (LST) has been used to model the geographic distribution of mosquito species in Africa (Rogers et al., 2002). MODIS LST and NDVI, in combination with precipitation data derived from the Tropical Rainfall Monitoring Mission Microwave Imager (TRMM-TMI) have been used to predict malaria risk in Afghanistan (Adimi et al., 2010). Many other studies have applied land cover and land use data derived from remote sensing to identify potential mosquito habitats (Brown et al., 2008; Chuang et al., 2011; Clennon et al., 2010; Masuoka et al., 2003). Multiple sources of remote sensing data were used to identify negative associations of

elevation and urbanization and a positive association of LST with West Nile virus infection rate in mosquitoes in Los Angeles (Liu & Weng, 2012).

A valuable potential application of remote sensing in public health is the development of early warning systems that forecast potential for disease outbreaks based on measurements of antecedent environmental risk factors. For example, an experimental vectorial capacity model has been developed using remotely sensed rainfall and temperature data to forecast malaria risk in the semiarid and highland regions in Africa (Ceccato et al., 2012). However, a major limitation of remote sensing is that most spaceborne sensors currently used for disease modeling and forecasting do not measure the proximal environmental variables that affect mosquito populations. For example, although mosquitoes are directly influenced by air temperature, most remotely-sensed temperature products measure the radiometric land surface (skin) temperature which is highly sensitive to thermal loading due to insolation, moisture status, and recent weather in addition to the bulk emissivity of the materials within the scene. As a result, land surface temperature may not be tightly correlated with the near surface air temperature recorded at weather stations (Vancutsem et al., 2010).

Rainfall estimates are available from satellite products including the TRMM-TMI sensor (Kummerow et al., 1998), and are frequently used in analyses of mosquito populations and mosquito-borne disease risk (Adimi et al., 2010). However, both the abundance and the quality of breeding sites depend on other factors besides precipitation, including the amount of soil moisture, soil characteristics, topography, land use, and evapotranspiration (Shaman & Day, 2005). Thus, it is often difficult to develop generalizable relationships between precipitation, mosquitoes, and mosquito-borne diseases (Landesman et al., 2007; Olson et al., 2009).

The NDVI provides an indicator of absorption of photosynthetically active radiation (400–700 nm), which is, in turn, a rough proxy of the amount of chlorophyll at the surface (Gitelson et al., 2003). Thus, the NDVI indirectly integrates multiple environmental variables including moisture, temperature, and vegetation structure. Although the NDVI tends to be a strong correlate of multiple ecological phenomena, they do not map simply to measures of plant biomass because they are sensitive to the effects of spatial and temporal variability in weather and climate with spatial variability in vegetative cover. Therefore, relationships between disease patterns and vegetation indices established in a particular region are difficult to extrapolate to other areas. To enhance the surveillance and prediction of mosquito-borne diseases, there is a need to develop remote sensing products that provide more effective measurements of near-ground temperature, humidity, soil moisture, and standing water.

A daily global land surface parameter database was developed from the NASA Advanced Microwave Scanning Radiometer on the Earth Observing System (AMSR-E), and provides several environmental variables that are potentially relevant to mosquito ecology, including near-surface air temperature, surface soil moisture, fractional open water cover, and estimates of vegetation canopy opacity to microwave emissions at three microwave frequencies (Jones et al., 2010; Jones & Kimball, 2010). Advantages of microwave radiometry include the ability to estimate global surface air temperature and other parameters day or night, and under cloudy, non-precipitating, non-frozen conditions. Compared to remote sensing based on visible and near-infrared wavelengths, lower-frequency satellite microwave remote sensing is largely insensitive to atmospheric contamination, resulting in a larger signal-to-noise ratio and the potential for near-daily global observations of the land surface. The AMSR-E land parameter data offer an opportunity to improve the environmental modeling and early warning of WNV risk by

testing the effectiveness of new environmental measurements that are directly relevant to the breeding habitats and population dynamics of mosquitoes.

Our study focused on the population dynamics of two mosquito species that are considered important in the northern Great Plains region of North America. *Culex tarsalis* Coquillet is the major vector of WNV in this region (Bell et al., 2005; Bolling et al., 2007). *Aedes vexans* Meigen is a nuisance mosquito and can potentially serve as a bridge vector of WNV (Turell et al., 2005). Previous research has highlighted the importance of the Northern Great Plains as a region of consistently high WNV risk and quantified influences of climate and land cover on spatial patterns of WNV risk (Chuang et al., 2012; Wimberly et al., 2008). Meteorological variables measured using weather stations have also been identified as important drivers of mosquito abundance, with *Cx. tarsalis* most sensitive to temperature and *Ae. vexans* most sensitive to rainfall (Chuang et al., 2011).

The present study expanded upon this previous work by hypothesizing that land surface parameters derived from AMSR-E data would quantify environmental factors relevant to mosquito abundance and, therefore, improve the accuracy of mosquito abundance models compared to standard meteorological measurements from weather stations. Major study objectives included: (1) Compare the environmental models of the population dynamics of two mosquito species in Sioux Falls, South Dakota using predictor variables from *in situ* daily weather station measurements and AMSR-E daily land surface parameter retrievals; (2) Determine which environmental variables were the most important predictors of each mosquito species (*Culex tarsalis* and *Aedes vexans*); and (3) Validate the selected models against local population measurements and generate a predicted map of mosquito climatic suitability across eastern South Dakota.

## 2. Material and methods

### 2.1 Study area

Eastern South Dakota is located in the northern Great Plains region of the United States and is defined as the portion of the state lying east of the Missouri River. Major physiographic zones include the Coteau des Prairies, James River Valley, and Missouri Coteau. The regional landscape has generally low relief and glacial deposits have resulted in clay-rich soils that develop impermeable surfaces that are favorable for temporary pooling of water. Sioux Falls is the largest city in South Dakota with a population of 153,888 (U.S. Census 2010). It is located at the southern tip of the Couteau des Prairies in the valley of the Big Sioux River and is surrounded by an agricultural landscape dominated by croplands dedicated to maize and soy production, pastures, and hayfields.

### 2.2 Mosquito sampling

*Culex tarsalis* and *Aedes vexans* samples were collected by the city of Sioux Falls, which is the major metropolitan area in south eastern South Dakota (Figure 1). The Sioux Falls Health Department maintains multiple CDC $CO_2$-baited light traps (John W. Hock Company, Gainesville, FL) during the mosquito season from May to September. The numbers of traps varied from 20 to 40 traps from 2005 to 2010 and 17 traps that were consistently operated during the study period were included in the analysis. Mosquito traps were set every day from Monday to Thursday and the samples were collected the next day (Tuesday to Friday). Mosquito species were identified by staff according to their morphological characteristics. The natural log-transformed (raw trap count+ 1) was applied to estimate the daily mosquito number per trap night and then the weekly mean results were summarized from all traps. Similar mosquito collection procedures were used in Brookings County, approximately 90 km to the north of Sioux Falls (Figure 1). In order to validate the

final models, we used mosquito data summarized from five traps in Brookings County to examine whether model predictions could be applied to a different location within the same region.

### 2.3 Satellite data

The primary remote sensing data for this study were daily global land surface parameters derived from AMSR-E (Jones & Kimball, 2010). This product provided daily, global coverage over the time period from June 19, 2002 through December 31, 2010, at a spatial resolution of 25 km. Near-surface (~2 m height) air temperature, fractional open water cover, surficial soil moisture, and vertically integrated atmospheric water vapor were estimated from brightness temperatures at 6.9, 10.7, and 18.7 GHz frequencies and horizontal and vertical polarizations under classified non-frozen conditions (Kim et al., 2011).

The AMSR-E derived air temperatures have been found to be strongly correlated ($r>=0.88$) with daily surface air temperature records from Northern Hemisphere weather stations of the World Meteorological Organization (Jones et al., 2010). A forward model sensitivity analysis indicated that the retrieval algorithm effectively resolves the vegetation opacity seasonal cycle over a majority of global vegetated land areas, with mean retrieval relative error (expressed as a percent of retrieved vegetation opacity) </=30% for vegetation opacity levels between 0.5–1.5, which effectively covers ~66% of the global vegetated land area. The expected retrieval error is closer to ~+/−20% within the SD study domain. The vegetation opacity results were also favorably correlated ($p<0.01$) with MODIS NDVI/EVI and LAI parameters, with correlations for global vegetation types characteristic of the SD domain ranging from 0.6 (cropland/natural veg), 0.6 (grassland) and 0.62 (Savanna) (Jones et al., 2011).

A forward model sensitivity analysis showed expected AMSR-E fractional water retrieval uncertainty within +/−4.1% (RMSE spatial classification accuracy), with sufficient accuracy to resolve regional inundation patterns and seasonal to annual variability (Watts et al., unpublished data). This study also indicated that the fractional water maps reflected strong microwave sensitivity to sub-grid scale open water variability and compared favorably ($0.84<r<0.92$) with alternative, static fractional water maps derived from finer scale (30-m to 250-m resolution) Landsat and combined MODIS and SRTM (MOD44W) data. The same study also reported favorable temporal correspondence ($0.71<r<0.87$) between the AMSR-E fractional inundation retrievals and regional wet/dry cycles inferred from northern basin discharge records.

The AMSR-E soil moisture retrievals have previously been validated through comparisons with in situ soil moisture network measurements and antecedent moisture indices derived from independent satellite (TRMM-TMI) precipitation data. These results show that the soil moisture retrievals are responsive to rapid precipitation wetting and drying cycles within 2–5 days in accordance with AMSR-E brightness temperature (10.7 and 6.9 GHz) sensitivity to surface (<2 cm depth) soil moisture conditions (Jones et al. 2009); soil moisture retrieval accuracy is reduced at higher vegetation biomass levels, with effective retrieval saturation above ~1.2–1.4 vegetation opacity, which is consistent with previous AMSR-E soil moisture validation studies (Njoku and Chan, 2006). Previous intensive validation studies for AMSR-E soil moisture products derived using four different retrieval algorithms indicate mean bias adjusted retrieval accuracies of 0.082+/−0.05 (RMSE, $m^3\ m^{-3}$) and mean correlation coefficients of 0.671+/−0.10 based on product comparisons against intensive in situ soil moisture network observations from four USDA ARS experimental watersheds within the continental USA (Jackson et al., 2010).

The major parameters of interest for mosquito-borne disease modeling and forecasting are the daily air temperature minima and maxima at 2 m height (TA), fractional cover of open water (FW), surficial soil moisture at ≤ 2 cm soil depth (MV), and microwave vegetation opacity (TC). In this study, the daily environmental indicators were averaged from the AMSR-E ascending (afternoon) and descending (morning) overpass images of each single day and then the weekly averages were calculated from the daily summarized measurements. To compare the satellite retrievals against weekly mosquito data from Sioux Falls, the average values of the AMSR-E derived environmental indicators were summarized from 5, 25-km resolution pixels that covered the entire study area. The automated data processing of the time series (2005–2010) of satellite images was carried out using Python 2.6 (Python Software Foundation) scripts and ERSI ArcGIS geoprocessing functions. All map layers were reprojected to a consistent Albers Equal Area (AEA) projection.

### 2.4 Weather station data

Meteorological data was acquired from the first-order weather station (KFSD) at the Sioux Falls Regional Airport (N 43 °34', W 96°43') in the northern part of the city. The daily average weather variables, including temperature, relative humidity, and total precipitation were computed from the hourly measurements. In order to match the temporal scale of the AMSR-E and mosquito data, weekly summaries were computed and used in the analysis.

### 2.5 Statistical Analysis

We used statistical models to explore the effects of lagged environmental variables on temporal patterns of observed mosquito abundance. However, because different time lags of the same environmental variable are typically highly correlated, severe multicollinearity problems often arise when classical linear regression approaches are applied. To avoid this dilemma, we used polynomial distributed lag (PDL) models, which constrain the lagged parameter estimates to fit polynomial functions so that estimation problems will be reduced (Almon, 1965). The PDL method was originally proposed in the field of econometrics and has been applied in epidemiology and environmental health only recently (Hu et al., 2006; Schwartz, 2000). The equations of the PDL model are

$$y_t=\alpha+\Sigma_{i=0}^{p}\beta_i x_{t-i}+\gamma z_t+\mu_t \quad (1)$$

$$\beta_i=\alpha_0+\Sigma_{j=0}^{d}\alpha_j f_j(i) \quad (2)$$

where $y_t$ is the independent variable at time $t$, $\alpha$ is the intercept, $x_t$ is the independent variable at lag $i$, $z_t$ indicates a simple covariate, $\gamma$ is the coefficient of a simple covariate, $\beta_i$ are the coefficients of the lag values, and $\mu_t$ is an error term. The distribution of lagged effect is modeled by lag polynomials and the coefficients $\beta_i$ are estimated from the equation 2, where $f_j(i)$ is a polynomial function of degree $j$ at the lag length $i$, and $\alpha_j$ is a coefficient estimated from the data. In the AMSR-E model, the $x_t$ included temperature, water fraction, soil moisture, and vegetation opacity inputs. In the weather station model, the $x_t$ included temperature, relative humidity, and precipitation inputs.

A first-order autoregressive term was also included in the models to account for the temporal correlations of the mosquito population in consecutive weeks. We also controlled for seasonality by including a sinusoidal term (sin ($2\pi$*week/52)) in the models as a simple covariate. The dependent variable was the natural log-transformed weekly mosquito abundance per trap/night computed as the mean abundance of all 17 mosquito traps in the Sioux Falls study area.

We fit two sets of models for each of the two mosquito species. The independent variables in the first set of models were the environmental measurements from the AMSR-E land surface parameters product (TA, FW, MV, and TC). The independent variables in the second set of models were derived from the weather station data (temperature, precipitation, and relative humidity). Each of the independent variables was computed for lags of zero, one, two, and three weeks. We considered all possible combinations of environmental variables for both the AMSR-E models (15 models) and the weather station models (7 models). A second-degree polynomial was determined to be sufficient for modeling variability in the parameters across these lags.

We compared the performance of the models using the corrected Akaike's Information Criterion (AICc), which penalized for the number of parameters and finite sample size. The model performance was evaluated by comparing the resulting Akaike weights. A lower AICc indicates a better fit of the model penalized for the number of model parameters, so we determined the best model with the minimum AICc among the candidate models. The Akaike weights provide information about the relative weight of evidence for candidate models and are a useful performance indicator especially when there are multiple competing models (Burnham & Anderson, 2002). We used data from 2005 to 2010 for model fitting. A leave-one-out cross-validation method was used to evaluate prediction accuracy of the best-fitting models by sequentially dropping one year at a time, fitting the model with the remaining years, predicting mosquito abundances based on the environmental variables for the year that was withheld, and computing the root mean square error (RMSE) to evaluate the prediction accuracy.

The best-fitting AMSR-E models were also used to generate maps of climatic suitability for both mosquito species across all of eastern SD. To produce these maps, we used the environmental variables included in the best-fitting AMSR-E models and applied equations 1 and 2 to the weekly variables for every 25 km pixel in South Dakota east of the Missouri River. We used the Brookings County mosquito survey data from 2008 to 2010 to test the ability of the best-fitting AMSR-E models to predict temporal variability in mosquito abundance at a different location within the region. Pearson's correlation coefficients were calculated to compare model predictions of climatic suitability and observed mosquito abundances. The first-order autoregressive term was included in our model fitting process; however, this information would not be available in a scenario where the aim is to predict mosquito abundance at unsampled locations. For this reason, the first-order autoregressive term was not included in the model validation process and climatic suitability was determined only by the environmental variables. All of the statistical models were fit using the SAS 9.2 using PDLREG procedure (SAS Institute Inc. Cary, NC).

## 3. Results

The total numbers of *Ae. vexans* and *Cx. tarsalis* mosquitoes captured from 2005 to 2010 were 387,277 and 90,273, respectively. The average natural log-transformed abundance varied from 0.92 to 2.19 per trap night for *Ae. vexans*, and from 0.42 to 1.21 per trap night for *Cx. tarsalis*.

The environmental variables derived from AMSR-E are shown in Figure 2 for eastern South Dakota. We compared the two sets of images which included four environmental variables in spring (March to May) and summer (June to August). 2009 was a relatively dry year (Mar-Aug total rainfall: 171.1 mm) compared to 2010 which was a relatively wet year (Mar-Aug total rainfall: 236.4 mm). The higher proportion of water fraction and wetter soil conditions in 2010 were captured by the AMSR-E variables, particularly in the spring (Figure 2).

The seasonal and interannual variability in the environmental variables derived from AMSR-E and the weather station during the study period (2005–2010) are shown in Figure 3. The seasonal patterns of air temperature from the two different data sources were highly correlated (r=0.94); however, higher air temperatures were obtained from AMSR-E than for the meteorological station data during the winter. Surface water fraction and soil moisture from AMSR-E were moderately correlated (r=0.62). There were much weaker correlations (r<0.25) between moisture variables from AMSR-E (soil moisture or water fraction) and moisture variables from the Sioux Falls weather station (precipitation and humidity), emphasizing the fact that these meteorological variables are not necessarily effective surrogates for surface wetness. The relatively high correlation between vegetation opacity and temperature (r=0.72) highlighted the close linkage between land surface phenology and seasonal patterns of air temperature.

For *Ae. vexans*, the best-fitting AMSR-E model included water fraction and temperature (AICc=349.41, weight=0.82, Table 1). In this model, the abundance of *Aedes vexans* was positively associated with temperature at current and one week lags, and water fraction at two to three week lags (Table 2). The best fitting weather station model included temperature and precipitation as independent variables (AICc=356.82, weight=0.47), although two closely competing models included temperature alone (AICc=357.99, weight=0.26) and temperature and humidity (AICc=358.42, weight=0.21) (Table 1). In the best-fitting weather station model, *Aedes vexans* abundance had significant associations with temperature at zero and one week lags and precipitation at one, two, and three week lags. The fit of the best AMSR-E model was better than the fit of the best weather station model (AICc= 349.41 vs. 356.82, Table 1).

*Culex tarsalis* showed different associations with environmental variables compared to *Aedes vexans*. The best-fitting *Cx. tarsalis* model included temperature and vegetation opacity (AICc=189.26, weight=0.63, Table 3). For the weather station models, only temperature was included in the best-fitting model (AICc=213.02, weight=0.55) although both temperature and humidity were included in a closely competing model (AICc=214.15, weight=0.31) (Table 3). The lagged effects of the environmental variables were also slightly different compared to the *Ae. vexans* models. The best AMSR-E model has positive effects of temperature at one and two week lags and vegetation opacity at zero and one week lags (Table 2). Similar to the results for *Ae. vexans*, the best AMSR-E model had a better fit than the best weather station model (AICc=189.26 vs. 213.02, Table 3).

The model comparison exercise showed that the AMSR-E models had better fits than the weather station models, and the fit of the AMSR-E models was illustrated by graphs of the observed and fitted values of mosquito abundance (Figure 4). The models for both *Ae. vexans* and *Cx. tarsalis* were able to capture the main seasonal patterns and interannual variability of mosquito abundance, although the fitted values tended to underestimate the highest peaks.

### 3.1 Model validation

The cross validated RMSE was similar for the AMSR-E and weather station models, although the RMSE values for the AMSR-E model were lower than for the weather station models in most years (Figure 5). RMSE values were consistently lower for *Cx. tarsalis* than for *Ae. vexans* except for 2010, when the RMSE values for both species were higher than in other years. The correlation coefficients between predicted and observed values in Brookings, SD were 0.76 for *Ae. vexans* and 0.52 for *Cx. tarsalis*. These model evaluations demonstrated a strong potential for predicting mosquito populations in future years in Sioux Falls, and a comparatively modest accuracy for predicting temporal variability in mosquito abundance at other locations.

### 3.2 Climatic Suitability Maps

Maps of climatic suitability in 2010 were generated for both species using the best AMSR-E models (Figure 6). The weekly time-series risk maps reflected the influences of different environmental parameters in the models. The effects of temperature were significant in both models and were reflected in strong seasonal trends of climatic suitability. For example, the decrease in predicted *Cx. tarsalis* abundance from week 22 to week 24 reflected cooler temperatures in early June compared to late May across most of eastern South Dakota. Water fraction and vegetation opacity captured different spatial patterns of environmental variability that are reflected in the geographic distributions of the two species.

## 4. Discussion and Conclusions

This study examined the fit and predictive capabilities of statistical models of *Ae. vexans* and *Cx. tarsalis* abundance using environmental measurements derived from the AMSR-E, a passive microwave spaceborne sensor, and local weather station data in Sioux Falls, SD. The results indicated that models based on the AMSR-E products fit the data better than models based on weather station data and made more accurate predictions. Furthermore, the distinctive mosquito ecologies of *Ae. vexans* and *Cx. tarsalis* were reflected by the different responses to the environmental variables in the AMSR-E models. This finding emphasizes that the AMSR-E derived land parameters are not simply proxies of the weather station measurements but instead provide unique environmental measurements that may be more useful for predicting mosquito activity.

The environmental parameters derived from the AMSR-E are not limited to meteorological variables and therefore provide additional information about vegetation characteristics and surface moisture conditions relevant to vector ecology. For example, *Aedes vexans* is a well-known floodwater mosquito: its population increases very quickly in response to precipitation (Schafer & Lundstrom, 2006). Female *Aedes vexans* tend to lay eggs in places that have high potential to be inundated after rainfall, and large numbers of these eggs hatch immediately after rainfall enlarges the sizes of these temporary pools (Becker et al., 2003). However, precipitation is not always a reliable indicator for ephemeral water pools, and the creation of water pools still relies on other factors like evaporative demand, surface drainage and antecedent soil moisture conditions.

The water fraction detected by the AMSR-E was an effective indicator for *Ae. vexans* abundance because it provided a direct measurement of the availability of temporal surface water bodies produced by rainfall. This finding is similar to the study in Florida which identified the positive association between the surface wetness and *Ae. vexans* population using dynamic hydrology models (Shaman et al., 2002). Air temperature is another important factor influencing *Ae. vexans* abundance. In general, larvae of this species will hatch from the eggs if the ambient temperature exceeds 9 °C and the larvae development rate will increase with temperature (Becker et al., 2003). Thus, the short term effect of temperature (lag 0 and lag 1) and slightly longer term effect of water fraction (lag 2 and lag 3) in the AMSR-E model reflected the ecological characteristics of *Ae. vexans*.

*Culex tarsalis* has a different ecological niche than *Aedes vexans*. In the northern Great Plains, this species tends to be abundant near perennial grasslands and hayfields (Chuang et al., 2011). In contrast to *Ae. vexans, Cx. tarsalis* species does not respond rapidly either to precipitation or the proportion of open water on the ground. Our models demonstrated that vegetation opacity and temperature are the two most important factors for predicting population numbers for this species. Vegetation opacity, like NDVI, is a composite indicator of temperature and moisture conditions which potentially influence mosquito activity and larval habitats. Many previous studies have used vegetation indices as biological indicators

of vector activity or disease incidence (Anyamba et al., 2001; Gomez-Elipe et al., 2007; Liu & Chen, 2006). Other potentially important variables correlated to the ecology of this species are not included in the models. For instance, the survival probability of overwintering adults may be determined by the environmental conditions during the preceding winter, which may affect the initial population size of *Cx. tarsalis* that emerges in the spring (Reisen et al., 2008).

Although we have parameterized and applied our models for mosquito species in a relatively small region of South Dakota (3606 $km^2$), our results also provide insights into how they might be applied more broadly. The cross-validation of model predictions in Sioux Falls suggests a strong potential for modeling and forecasting temporal patterns of mosquito abundance at sites where sufficient data is available model calibration. The maps of climatic suitability are based on spatial extrapolation of temporal associations with environmental drivers from a single site, and thus serve mainly as a demonstration of the potential for modeling spatio-temporal fluctuations in mosquito abundance across larger areas. Future research efforts will focus on developing risk maps using spatially extensive datasets on vector abundance and disease incidence.

Globally data availability and automated data retrieval are two of the major advantages of remote sensing technique so our models can be applied to different geographic regions subject to vector-borne diseases. In most parts of the world, vector surveillance systems and ground-level environmental data are usually very limited. Remote sensing techniques can play a very important role in monitoring and predicting vector activity and disease incidence. For example, *Ae. vexans* is also an important vector for Rift Valley Fever (RVF) in sub-Saharan and North Africa, and a recent study showed the associations between rainfall and RVF transmission risk in Senegal (Vignolles et al., 2009). Integrating AMSR-E and similar satellite microwave remote sensing data could enhance the mapping and forecasting of vector distributions in this region.

A limitation of the AMSR-E data is the relatively coarse spatial resolution (25 km) of the passive microwave land parameter retrievals. However, this limitation is offset by relatively high (1–2 days) temporal fidelity and the ability to collect data at night and under cloudy conditions. These advantages are particularly valuable in tropical regions, which have both significant cloud cover and high burden of mosquito-borne diseases. Although we can also do a reasonably good job mapping surface water with VNIR sensors like Landsat and MODIS, neither of these sensors would be able to provide as much data over time as AMSR-E under typical weather conditions. Although AMSR-E data cannot be used to identify the precise spatial locations of mosquito breeding sites, the spatial scale should suffice to capture climatic anomalies that tend to be manifested at much larger spatial scales. Another limitation of the satellite derived temperatures is due to retrieval gaps during classified frozen or snow covered land surface conditions, leading to an apparent warm bias in winter. Additional gap filling and bias correction using other sources of air temperature data may need to be incorporated in applications that require accurate temperatures during winter.

In this study, we have demonstrated the usefulness of multiple environmental indictors derived from passive microwave radiometry which can provide improved environmental metrics for mosquito-borne disease applications compared with ground-level weather stations. The AMSR-E sensor on Aqua ceased effective operations in October 2011 due to a malfunction of the sensor antenna spin mechanism. However, another AMSR sensor was launched in May 2012 onboard the JAXA GCOM-W satellite, enabling the continuation of global land parameter retrievals and future applications for modeling and forecasting mosquito-borne diseases. In the future, satellite passive microwave radiometry can be

applied to determine the seasonal timing of environmental indicators at broader geographic extents and more sophisticated models can be developed for disease forecasting. These data also could be integrated with other remote sensing sources to take advantage of the high temporal consistency of observations from passive microwave radiometry and the higher spatial resolution of other datasets.

## Acknowledgments

We thank the staff of the Sioux Falls Health Department and South Dakota State University who assisted with the collection of mosquito surveillance data. Funding for this work was provided by the NASA Applied Science Program (grant NNX11AF67G) and the National Institutes of Health, National Institute of Allergy and Infectious Diseases (grant R01-AI079411).

## References

Adimi F, Soebiyanto RP, Safi N, Kiang R. Towards malaria risk prediction in Afghanistan using remote sensing. Malaria Journal. 2010; 9:125. [PubMed: 20465824]

Almon S. The Distributed Lag Between Capital Appropriations and Expenditures. Econometrica. 1965; 33(1):178–196.

Anyamba A, Linthicum KJ, Tucker CJ. Climate-disease connections: Rift Valley Fever in Kenya. Cadernos de saude publica. 2001; (17 Suppl):133–140. [PubMed: 11426274]

Beck LR, Lobitz BM, Wood BL. Remote sensing and human health: new sensors and new opportunities. Emerging Infectious Diseases. 2000; 6(3):217–227. [PubMed: 10827111]

Becker, N.; Petric., D.; Zgomba, M.; Boase., C.; Dahl, C.; Lane, J.; Kaiser, A. Mosquitoes and their control. Kluwer Academic / Plenum Publisher; New York: 2003.

Bell JA, Mickelson NJ, Vaughan JA. West Nile virus in host-seeking mosquitoes within a residential neighborhood in Grand Forks, North Dakota. Vector-Borne and Zoonotic Diseases. 2005; 5(4):373–382. [PubMed: 16417433]

Bolling BG, Barker CM, Moore CG, Pape WJ, Eisen L. Seasonal patterns for entomological measures of risk for exposure to *Culex* vectors and West Nile virus in relation to human disease cases in northeastern Colorado. Journal of Medical Entomology. 2009; 46(6):1519–1531. [PubMed: 19960707]

Bolling BG, Moore CG, Anderson SL, Blair CD, Beaty BJ. Entomological studies along the Colorado Front Range during a period of intense West Nile virus activity. Journal of the American Mosquito Control Association. 2007; 23(1):37–46. [PubMed: 17536366]

Brown HE, Diuk-Wasser MA, Guan Y, Caskey S, Fish D. Comparison of three satellite sensors at three spatial scales to predict larval mosquito presence in Connecticut wetlands. Remote Sensing of Environment. 2008; 112(5):2301–2308.

Burnham, KP.; Anderson, DR. Model selection and multimodel inference : a practical information-theoretic approach. Springer; New York, London: 2002.

Ceccato P, Vancutsem C, Klaver R, Rowland J, Connor SJ. A vectorial capacity product to monitor changing malaria transmission potential in epidemic regions of Africa. Journal of tropical medicine. 2012; 2012:595948. [PubMed: 22363350]

Chuang TW, Hildreth MB, Vanroekel DL, Wimberly MC. Weather and land cover influences on mosquito populations in Sioux Falls, South Dakota. Journal of Medical Entomology. 2011; 48(3): 669–679. [PubMed: 21661329]

Chuang TW, Hockett CW, Kightlinger L, Wimberly MC. Landscape-level spatial patterns of west nile virus risk in the northern great plains. American Journal of Tropical Medicine and Hygiene. 2012; 86(4):724–731. [PubMed: 22492161]

Clennon JA, Kamanga A, Musapa M, Shiff C, Glass GE. Identifying malaria vector breeding habitats with remote sensing data and terrain-based landscape indices in Zambia. International Journal of Health Geographics. 2010; 9:58. [PubMed: 21050496]

Ebel GD, Rochlin I, Longacker J, Kramer LD. *Culex restuans* (Diptera: Culicidae) relative abundance and vector competence for West Nile Virus. Journal of Medical Entomology. 2005; 42(5):838–843. [PubMed: 16363169]

Gitelson AA, Gritz Y, Merzlyak MN. Relationships between leaf chlorophyll content and spectral reflectance and algorithms for non-destructive chlorophyll assessment in higher plant leaves. Journal of Plant Physiology. 2003; 160(3):271–282. [PubMed: 12749084]

Gomez-Elipe A, Otero A, van Herp M, Aguirre-Jaime A. Forecasting malaria incidence based on monthly case reports and environmental factors in Karuzi, Burundi, 1997–2003. Malaria Journal. 2007; 6:129. [PubMed: 17892540]

Gubler DJ. Resurgent vector-borne diseases as a global health problem. Emerging Infectious Diseases. 1998; 4(3):442–450. [PubMed: 9716967]

Hay SI, Lennon JJ. Deriving meteorological variables across Africa for the study and control of vector-borne disease: a comparison of remote sensing and spatial interpolation of climate. Tropical Medicine & International Health. 1999; 4(1):58–71. [PubMed: 10203175]

Hofmeister EK. West Nile virus: North American experience. Integrative Zoology. 2011; 6(3):279–289. [PubMed: 21910847]

Hu WB, Tong SL, Mengersen K, Oldenburg B. Rainfall, mosquito density and the transmission of Ross River virus: A time-series forecasting model. Ecological Modelling. 2006; 196(3–4):505–514.

Jackson TJ, M. H. Cosh R, Bindlish PJ, Stark DD, Bosch DC, Goodrich MS, Moran & J, Du. Validation of Advanced Microwave Scanning Radiomerter Soil Moisture Products. IEEE Transactions on Geoscience and Remote Sensing. 2010; 48(12):4256–4272.

Jones LA, Ferguson CR, Kimball JS, Zhang K, Chan SK, McDonald KC, Njoku EG, Wood EF. Daily land surface air temperature retrieval from AMSR-E: Comparison with AIRS/AMSU. IEEE Applied Earth Observations & Remote Sensing. 2010; 3(1):111–123.

Jones, LA.; Kimball, JS. Daily Global Land Surface Parameters Derived from AMSR-E. Boulder Colorado USA: National Snow and Ice Data Center. Digital Media. 2010. http://nsidc.org/data/nsidc-0451.html

Jones, LA.; Kimball, JS.; Podest, E.; McDonald, KC.; Chan, SK.; Njoku, EG. IEEE International Geoscence Remote Sensing Symposium. Cape Town, South Africa: 2009. A method for deriving land surface moisture, vegetation optical depth and open water fraction from AMSR-E.

Jones MO, Jones LA, Kimball JS, McDonald KC. Satellite passive microwave remote sensing for monitoring global land surface phenology. Remote Sensing of Environment. 2011; 115(4):1102–1114.

Kalluri S, Gilruth P, Rogers D, Szczur M. Surveillance of arthropod vector-borne infectious diseases using remote sensing techniques: a review. PLoS Pathogens. 2007; 3(10):1361–1371. [PubMed: 17967056]

Kim Y, Kimball JS, McDonald KC, Glassy J. Developing a Global Data Record of Daily Landscape Freeze/Thaw Status Using Satellite Passive Microwave Remote Sensing. IEEE Transactions on Geoscience and Remote Sensing. 2011; 49(3):949–960.

Kristan M, Abeku TA, Beard J, Okia M, Rapuoda B, Sang J, Cox J. Variations in entomological indices in relation to weather patterns and malaria incidence in East African highlands: implications for epidemic prevention and control. Malaria Journal. 2008; 7:231. [PubMed: 18983649]

Kummerow C, Barnes W, Kozu T, Shiue J, Simpson J. The Tropical Rainfall Measuring Mission (TRMM) sensor package. Journal of Atmospheric and Oceanic Technology. 1998; 15(3):809–817.

Landesman WJ, Allan BF, Langerhans RB, Knight TM, Chase JM. Inter-annual associations between precipitation and human incidence of West Nile virus in the United States. Vector-Borne and Zoonotic Diseases. 2007; 7(3):337–343. [PubMed: 17867908]

Liu H, Weng Q. Enhancing temporal resolution of satellite imagery for publichealth studies: A case study of West Nile Virus outbreak in Los Angeles in 2007. Remote Sensing of Environment. 2012; 117:57–71.

Liu J, Chen XP. Relationship of remote sensing normalized differential vegetation index to Anopheles density and malaria incidence rate. Biomedical and Environmental Sciences. 2006; 19(2):130–132. [PubMed: 16827184]

Machault V, Vignolles C, Pages F, Gadiaga L, Gaye A, Sokhna C, Trape JF, Lacaux JP, Rogier C. Spatial heterogeneity and temporal evolution of malaria transmission risk in Dakar, Senegal,

according to remotely sensed environmental data. Malaria Journal. 2010; 9:252. [PubMed: 20815867]

Masuoka PM, Claborn DM, Andre RG, Nigro J, Gordon SW, Klein TA, Kim HC. Use of IKONOS and Landsat for malaria control in the Republic of Korea. Remote Sensing of Environment. 2003; 88(1–2):187–194.

Njoku EG, Chan SK. Vegetation and surface roughness effects on AMSR-E land observations. Remote Sensing of Environment. 2006; 100(2):190–199.

Olson SH, Gangnon R, Elguero E, Durieux L, Guegan JF, Foley JA, Patz JA. Links between Climate, Malaria, and Wetlands in the Amazon Basin. Emerging Infectious Diseases. 2009; 15(4):659–662. [PubMed: 19331766]

Reisen WK, Cayan D, Tyree M, Barker CM, Eldridge B, Dettinger M. Impact of climate variation on mosquito abundance in California. Journal of Vector Ecology. 2008; 33(1):89–98. [PubMed: 18697311]

Rogers DJ, Randolph SE, Snow RW, Hay SI. Satellite imagery in the study and forecast of malaria. Nature. 2002; 415(6872):710–715. [PubMed: 11832960]

Schafer ML, Lundstrom JO. Different responses of two floodwater mosquito species, *Aedes vexans* and *Ochlerotatus sticticus* (Diptera: Culicidae), to larval habitat drying. Journal of Vector Ecology. 2006; 31(1):123–128. [PubMed: 16859100]

Schwartz J. The distributed lag between air pollution and daily deaths. Epidemiology. 2000; 11(3): 320–326. [PubMed: 10784251]

Shaman J, Day JF. Achieving operational hydrologic monitoring of mosquitoborne disease. Emerging Infectious Diseases. 2005; 11(9):1343–1350. [PubMed: 16229760]

Shaman J, Stieglitz M, Stark C, Le Blancq S, Cane M. Using a dynamic hydrology model to predict mosquito abundances in flood and swamp water. Emerging Infectious Diseases. 2002; 8(1):6–13. [PubMed: 11749741]

Trawinski PR, Mackay DS. Meteorologically conditioned time-series predictions of West Nile virus vector mosquitoes. Vector-Borne and Zoonotic Diseases. 2008; 8(4):505–521. [PubMed: 18279008]

Turell MJ, Dohm DJ, Sardelis MR, Oguinn ML, Andreadis TG, Blow JA. An update on the potential of north American mosquitoes (Diptera: Culicidae) to transmit West Nile Virus. Jounal of Medical Entomology. 2005; 42(1):57–62.

Vancutsem C, Ceccato P, Dinku T, Connor SJ. Evaluation of MODIS land surface temperature data to estimate air temperature in different ecosystems over Africa. Remote Sensing of Environment. 2010; 114(2):449–465.

Vignolles C, Lacaux JP, Tourre YM, Bigeard G, Ndione JA, Lafaye M. Rift Valley fever in a zone potentially occupied by *Aedes vexans* in Senegal: dynamics and risk mapping. Geospatial Health. 2009; 3(2):211–220. [PubMed: 19440963]

Watts J, Kimball JS, Jones LA, Schroeder R, McDonald KC. Satellite microwave remote sensing of contrasting surface water inundation changes within different pan-Arctic permafrost zones. Remote Sensing of Environment. Unpublished results.

World Health Organization. Malaria. 2009a; Vol WHO Fact Sheet No. 94.

World Health Organization. Dengue and dengue hemorrhagic fever. 2009b; Vol WHO Fact Sheet NO. 117.

Wimberly MC, Hildreth MB, Boyte SP, Lindquist E, Kightlinger L. Ecological niche of the 2003 west nile virus epidemic in the northern great plains of the United States. PLoS One. 2008; 3(12):e3744. [PubMed: 19057643]

**Highlights**

- Mosquito abundance was modeled using passive microwave data from the AMSR-E sensor.
- Models based on AMSR-E were more accurate than models based on meteorological data.
- Surface water, vegetation opacity, and air temperature predicted mosquito dynamics.
- Variability in mosquito climatic suitability was mapped in space and over time.

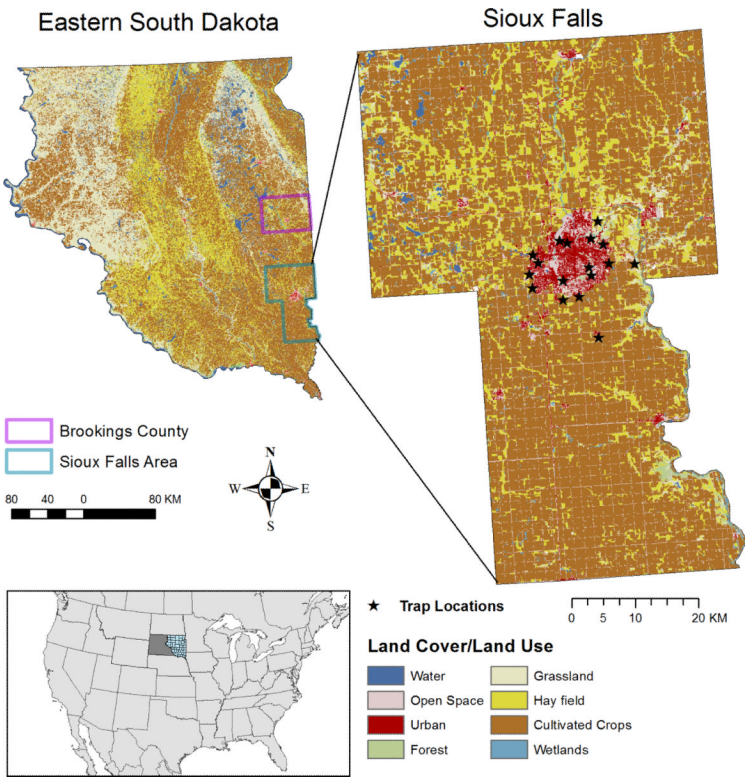


**Figure 1.**
Location of eastern South Dakota and the Sioux Falls study area. The land cover map for Sioux Falls is from the National Land Cover Dataset 2001.

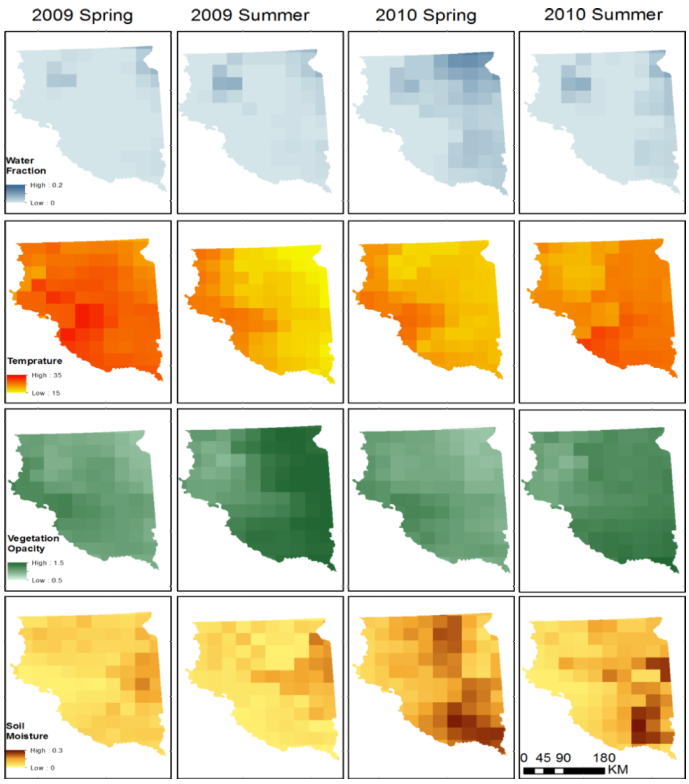


**Figure 2.**
Environmental parameters derived from the AMSR-E data in spring (average of March, April, and May) and summer (average of June, July, and August) in eastern South Dakota, 2009–2010.

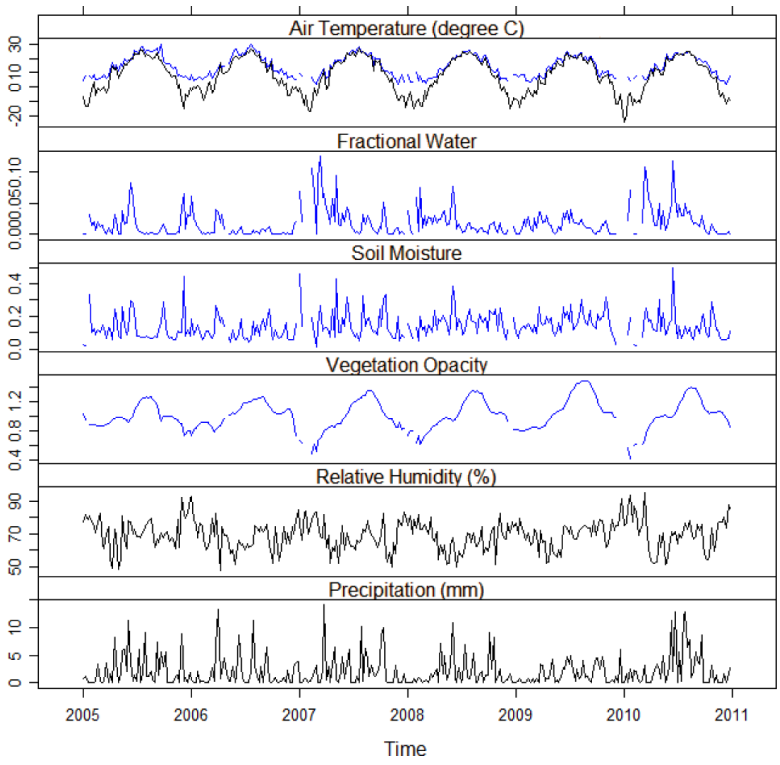


**Figure 3.**
Weekly environmental variables derived from AMSR-E (blue line) and the Sioux Falls Regional Airport weather station (black line) within the Sioux Falls study area, 2005–2010.

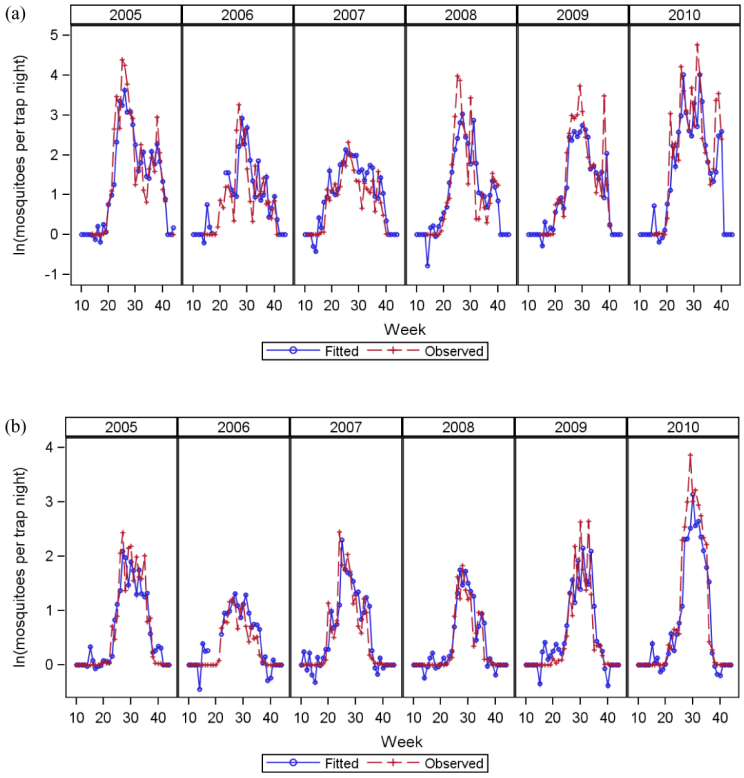


**Figure 4.**
Comparison of the predicted and observed values of (a) *Ae. vexans* and (b) *Cx. tarsalis* abundance using the best-fitting model based on AMSR-E data

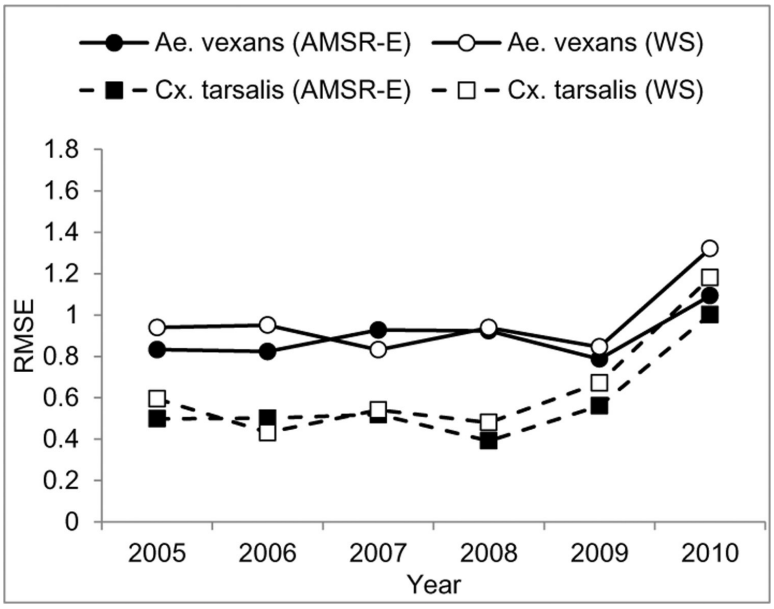


**Figure 5.**
Leave-one-out cross-validation of the best models from the two data sources for *Ae. vexans* and *Cx. tarsalis*.

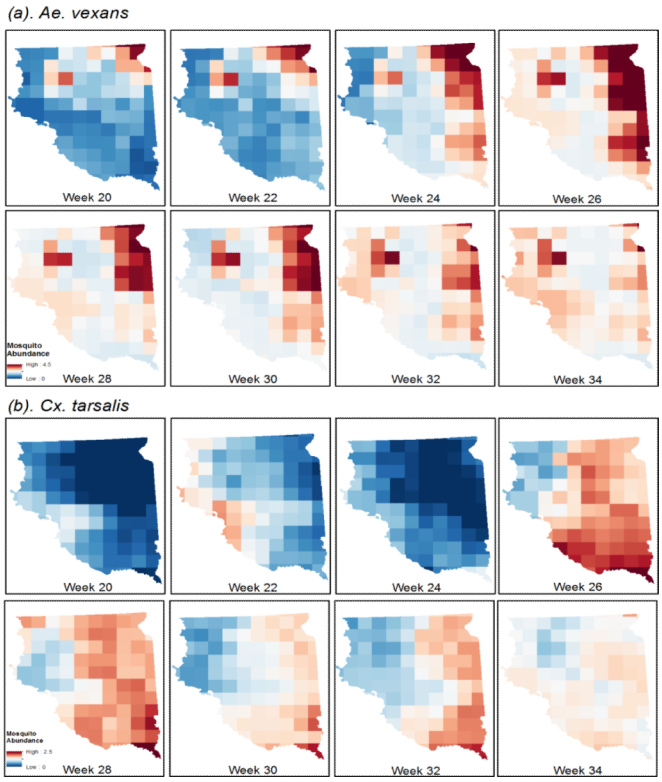


**Figure 6.**
Predicted maps of climatic suitability for (a) *Ae. vexans* and (b) *Cx. tarsalis* in eastern South Dakota, 2010.

*Remote Sens Environ*. Author manuscript; available in PMC 2013 October 01.

**Table 1**

Model selection results based on corrected Akaike's Information Criterion for *Aedes vexans*[#].

| Data Sources | *Ae. vexans* | | | | |
|---|---|---|---|---|---|
| | **Parameters** | **Variables** | **AICc** | **ΔAICc** | **Weight** |
| AMSR-E | 2 | TA, FW | 349.41 | 0.00 | 0.82 |
| | 2 | TA, MV | 354.35 | 4.94 | 0.07 |
| | 3 | TA, FW, MV | 354.72 | 5.31 | 0.06 |
| | 1 | TA | 356.34 | 6.93 | 0.03 |
| | 3 | TA, FW, TC | 356.86 | 7.45 | 0.02 |
| | 3 | TA, MV, TC | 359.16 | 9.75 | 0.01 |
| Weather Station | 2 | TA, PREC | 356.82 | 0.00 | 0.47 |
| | 1 | TA | 357.99 | 1.17 | 0.26 |
| | 2 | TA, RH | 358.42 | 1.60 | 0.21 |
| | 3 | TA, RH, PREC | 361.23 | 4.41 | 0.05 |

TA: air temperature, MV: soil moisture, FW: water fraction, TC: vegetation opacity, RH: relative humidity, PREC: precipitation

[#]: Only the models with Akaike weight≥0.01 are listed in the tables

## Table 2

Parameter estimates for the best-fitting PDL models for *Aedes vexans* and *Culex tarsalis*.

| Variables | *Cx. tarsalis* | | *Ae. vexans* | |
|---|---|---|---|---|
| | **Beta** | **S.E.** | **Beta** | **S.E.** |
| *AMSR-E* | | | | |
| Air Temperature | | | | |
| Lag 0 | 0.000 | 0.012 | 0.1000 | 0.0188*** |
| Lag 1 | 0.033 | 0.009*** | 0.0439 | 0.0136** |
| Lag 2 | 0.032 | 0.009*** | 0.0096 | 0.0141 |
| Lag 3 | −0.005 | 0.012 | −0.0030 | 0.0202 |
| Water Fraction | | | | |
| Lag 0 | | | 4.2635 | 3.4491 |
| Lag 1 | | | 8.1982 | 2.4650*** |
| Lag 2 | | | 8.6141 | 2.5011*** |
| Lag 3 | | | 5.5111 | 2.9945 |
| Vegetation Opacity | | | | |
| Lag 0 | 3.131 | 1.381* | | |
| Lag 1 | 2.620 | 1.116* | | |
| Lag 2 | 0.012 | 1.151 | | |
| Lag 3 | −4.695 | 1.344** | | |
| *Weather Station* | | | | |
| Air Temperature | | | | |
| Lag 0 | 0.0162 | 0.0104 | 0.0814 | 0.0162*** |
| Lag 1 | 0.0317 | 0.0080*** | 0.0397 | 0.0122** |
| Lag 2 | 0.0294 | 0.0077*** | 0.0093 | 0.0120 |
| Lag 3 | 0.0092 | 0.0108 | −0.0099 | 0.0175 |
| Precipitation | | | | |
| Lag 0 | | | 0.0139 | 0.0167 |
| Lag 1 | | | 0.0354 | 0.0174* |
| Lag 2 | | | 0.0448 | 0.0176* |
| Lag 3 | | | 0.0420 | 0.0176* |

*** : p-value<0.001.

** : p-value<0.01,

* : p-value<0.05

**Table 3**

Model selection results based on corrected Akaike's Information Criterion for *Culex tarsalis*[#]

| Data Sources | *Cx. tarsalis* | | | | |
|---|---|---|---|---|---|
| | **Parameters** | **Variables** | **AICc** | **ΔAICc** | **Weight** |
| AMSR-E | 2 | TA, TC | 189.26 | 0.00 | 0.63 |
| | 4 | TA, FW, MV, TC | 191.72 | 2.46 | 0.18 |
| | 3 | TA, MV, TC | 192.10 | 2.84 | 0.15 |
| | 3 | TA, FW, TC | 195.94 | 6.68 | 0.02 |
| | 1 | TC | 197.40 | 8.14 | 0.01 |
| Weather Station | 1 | TA | 213.02 | 0.00 | 0.55 |
| | 2 | TA, RH | 214.15 | 1.13 | 0.31 |
| | 3 | TA, RH, PREC | 216.68 | 3.66 | 0.09 |
| | 2 | TA, PREC | 217.90 | 4.88 | 0.05 |

TA: air temperature, MV: soil moisture, FW: water fraction, TC: vegetation opacity, RH: relative humidity, PREC: precipitation

[#]: Only the models with Akaike weight ≥0.01 are listed in the tables